Cavity Soliton Laser Based on Mutually Coupled Semiconductor Microresonators

P. Genevet, S. Barland, M. Giudici, and J. R. Tredicce
Université de Nice Sophia Antipolis, Institut Non-Linéaire de Nice, UMR 6618, 06560 Valbonne, France
(Received 11 June 2008; published 18 September 2008)

We report on experimental observation of localized structures in two mutually coupled broad-area semiconductor resonators, one of which acts as a saturable absorber. These structures coexist with a dark homogeneous background and they have the same properties as cavity solitons without requiring the presence of a driving beam into the system. They can be switched individually on and off by means of a local addressing beam.

DOI: 10.1103/PhysRevLett.101.123905 PACS numbers: 42.65.Tg, 42.55.Px, 42.65.Pc, 42.79.Ta

Localized structures (LS) form in large aspect-ratio media where two or several solutions coexist in the parameter space (see, e.g., [1] for a recent review). Cavity Solitons (CS) are LS generated in a cavity filled with a non linear medium driven by a coherent injected field (holding beam, HB) where they appear as single bistable bright intensity peaks coexisting with a homogeneous background. Their existence and mutual independence in semiconductors have been experimentally demonstrated in microcavities operated as optical amplifiers [2,3] since a local perturbation in form of a beam coherent with the HB can be used for switching CS on and off independently [2,4]. The possibility to control their location and their motion by introducing phase or amplitude gradients in the holding beam suggests their use as mobile pixels for all-optical processing units. Indeed, in the last decade, CS in semiconductor have attracted a growing interest since they combine the bistability and plasticity properties with the advantages of semiconductor media in terms of fast response and small size. The application potential of CS has been evidenced with some first-principle demonstration of new all-optical devices exploiting CS properties for optical memories [5] and delay lines [6]. Nevertheless, the tight conditions required for CS stability in present experimental schemes hinders their application to non prototypical devices. A radical simplification could be achieved implementing the concept of Cavity Soliton Laser (CSL), i.e., a device generating CS without an external injection beam. Such a device would have tremendous advantages in terms of simplicity, robustness, and compactness. Some steps in this direction have been made recently with a scheme based on broad-area VCSEL submitted to frequency selective feedback [7]. However, even if no HB is present it appears that the stability of localized structures in this case depends critically on mechanical feedback alignment and on the detuning between the resonator and the external frequency selecting element. An alternative approach is provided by a laser with a saturable absorber. Indeed, this system is among the first ones theoretically shown to possess the necessary ingredients for the generation of localized structures in optics, called in this case dissipative autosolitons [8]. While this initial work was realized in the limit of fast materials [8,9], it was later extended to the case of finite relaxation times [9,10]. Finally, the case of slow absorber material (as would be the case for semiconductors) was examined in [11] and the case where the absorbing and gain media have equal response times has been studied in [12]. The authors of these last references show numerically that in a vertical cavity surface emitting laser (VCSEL) with saturable absorber, CS related to the existence of a modulational instability can be switched on and off by injecting a local optical perturbation.

Despite this extensive theoretical and numerical research, we are not aware of any experimental observation of CS using a saturable absorber in semiconductor laser. In this letter we show the experimental realization of a CSL based on two mutually coupled microresonators where one plays the role of an amplifier and the second of a saturable absorber. As we shall demonstrate below, this scheme allows a remarkably simple realization of a cavity soliton laser. We show that bistable solitary structures coexist with a dark homogeneous background and that they can be switched on and off independently by an incoherent beam. We believe that this demonstration opens the way towards implementations in very compact monolithic devices including both the amplifying and saturable absorber sections [13].

The lasers we use are two nominally identical VCSELs provided by ULM photonics. They are oxydized bottom-emitter VCSELs emitting around 975 nm [14]. Their transverse section is 200 μm. They are mounted in a mutually coupled configuration, where one laser is electrically biased above the transparency but below its standalone coherent emission threshold (L_1), while the other is biased below transparency (L_2). Each device package is temperature stabilized. In order to compensate the effects of diffraction during the propagation in the extended cavity (60 cm long to accommodate the optics) and to keep the system highly symmetric, we use identical collimators and identical lenses placed such that the two resonators are in a self imaging condition (see Fig. 1). This configuration allows to preserve the high Fresnel number required for the existence of LS [3]. A 20% reflection beam splitter is

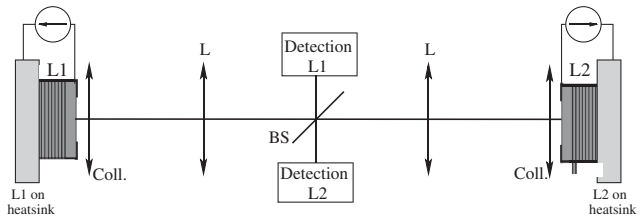

FIG. 1. Schematic drawing of the experiment. L_1: Laser above the transparency, L_2: Laser below the transparency, BS: beam splitter. Detection of L_1 (L_2) includes a CCD camera monitoring the near field of L_1 (L_2) and a fast detector to monitor the local temporal behavior.

inserted in the center of the cavity to extract two output beams from the system. Time-averaged near-field profiles of both resonators are simultaneously imaged on two charge-coupled device (CCD) cameras. The use of two CCD cameras allows us to check the output of the compound system in two different planes, located at each laser's active medium. In the detection path of laser L_1, an iris placed in an intermediate near-field plane enables to select a small area of the profile for pointlike temporally resolved detection. A photodetector Thorlabs PDA8GS (less than 100 ps rise time) coupled to a digital oscilloscope LeCroy Wavemaster 8600A (6 GHz analog bandwidth) monitors the output of this small portion of the L_1 profile.

The solitary VCSELs light intensity output as function of the pumping current (I_{L_1,L_2}) indicate that the uncoupled lasers have very similar standalone coherent emission thresholds $I^{\text{th}}_{L_1} \sim I^{\text{th}}_{L_2} \sim 400$ mA. The temperature control of each device is set such that the emission wavelength of laser L_1 is approximately 1 nm blue detuned with respect to laser L_2 when both devices are pumped by the same amount of current. In Fig. 2, left panel, we show the local intensity output of the compound system as a function of pumping current of L_1, (I_{L_1}), while I_{L_2} is kept fixed at a few mA, i.e., below the transparency pumping value. The monitored region has a diameter of about 20 μm and it is placed in the center of the device. When $I_{L_1} \leq 100$ mA (zone A in Fig. 2 left panel, the increase of emitted power is attributed to spontaneous emission, since the optical spectrum of the system does not show coherent emission. The first threshold ($I_{\text{th}} \sim 100$ mA, region B of Fig. 2, left panel) is reached when light linearly reflected on the output mirror of L_2 sufficiently reduces the losses of the compound system such that laser emission can be obtained. At that point, threshold reduction and coherent emission may therefore be attributed to losses reduction as is shown in conventional optical feedback experiments.

For, $I_{L_1} \geq 200$ mA (region C of Fig. 2, left panel) the power output of the compound system saturates and then decreases for increasing values of I_{L_1}. This happens when the longitudinal resonances of both cavities match and absorption in device L_2 takes place. The fact that the resonance frequencies of both devices match only for certain current values is due to the linear shift experienced by the laser frequency as a function of the pumping current due to Joule heating. The absorption by laser L_2 in region C of Fig. 2 has been verified by performing the same measurement with laser L_2 unpumped, which allows to verify the presence of a light induced current through the device, which is absent in regions A or B. Increasing further I_{L_1}, the intensity output remains constant at a low value. The optical spectra of this low intensity emission shows a broad band peak indicating that this state corresponds to spontaneous emission since absorption cut the feedback from L_2. Further increase of I_{L_1} above a critical value $I^c_{L_1}$ the local intensity jumps up to a high value. The optical spectrum associated to this state shows a well pronounced peak red-detuned with respect the spontaneous emission peak observed in the low level state. In the near-field profile this local transition of the intensity output corresponds to the formation of a bright single peak structure inside the monitored area. For larger I_{L_1} (region D of Fig. 2, left panel) the local intensity keeps increasing, while the near-field profile reveals the formation of multi peaked structures and extended patterns around the monitored region. If I_{L_1} is decreased the local intensity shows hysteresis demonstrating bistability between a low and a high emitted intensity state in the region monitored by the detector.

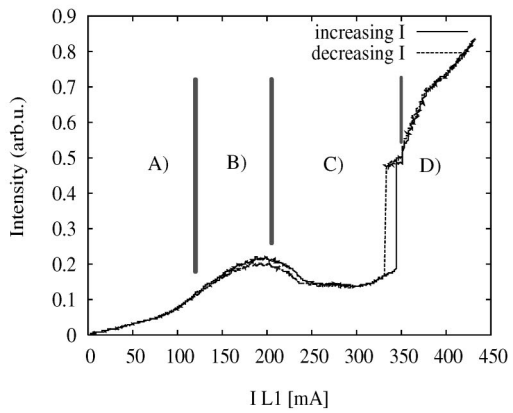

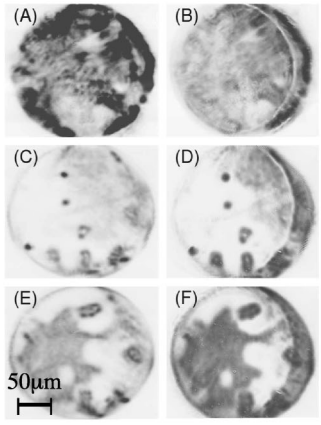

FIG. 2. Left: Local intensity output emitted by the system when scanning I_{L_1} with all the other parameters constant. (A) below threshold, (B) lasing by feedback, (C) absorption by L_2, bistable behavior, (D) pattern formation. Right: Near field of both devices. Dark areas correspond to high intensities. (a), (b) Near-field image of L_1 (L_2), before the interaction ($I_{L_1} = 180$ mA), (c), (d) Near field of L_1 (L_2), in the absorption zone ($I_{L_1} = 358$ mA), (e), (f) Near field of L_1 (L_2), when the pattern is developed ($I_{L_1} = 365$ mA). L_2 is slightly shifted on the left.

We note that while the data shown in Fig. 2 were obtained for a particular setting of the temperature of each device's substrate, equivalent results may be obtained for different temperature and current settings provided a number of conditions are satisfied. First of all, if device L_2 is pumped at a too high value, we made no observation of the bistable response of the system. Second, if L_1 is initially red-detuned with respect to L_2, these results wont be observed since both devices will not be resonant for any current value of L_1. The essential conditions are therefore an initial detuning allowing for current induced tuning of L_1 towards the resonance of L_2 when L_2 is kept in an absorbing regime. An additional condition is that if the suitable tuning condition is obtained for a too low value of pumping of device L_1 (pumping of device L_2 being kept constant) the total amount of field in the compound system does not seem to reach the saturation value. In this case, although the effects of absorption in L_2 can clearly be identified, no bistable behavior was observed. We expect, however, that this condition, related to the saturation fluence of device L_2, could also be satisfied by applying a demagnification factor in the imaging of device L_1 on device L_2 in our setup or decreasing the reflectivity of the central beam splitter.

A detailed study of required conditions has been performed and will be presented elsewhere, but for now we underline that provided that the previous conditions are fulfilled, the data shown on Fig. 2 can be obtained for different settings of device temperatures and currents, with I_{L_2} allowing to tune the amount of absorption in the system. As an order of magnitude, the results presented here could be obtained for a broad range of temperature settings leading to the bistability cycle being observed for currents in L_2 ranging from 5 to 30 mA and currents in L_1 ranging from 120 to 380 mA. We note that obtaining suitable conditions does not involve mechanical tuning, which is an advantage from an applicative standpoint.

In Fig. 2, right panel, we show the near-field transverse profiles of L_1 and L_2 for different values of I_{L_1}, while I_{L_2} is kept constant at 15 mA. As discussed previously, in the self imaging scheme configuration, L_1 and L_2 are placed on self-conjugate planes with a magnification of one. In order to monitor the absorption, the devices are slightly shifted with respect to each other in the horizontal direction. This way, a small portion close to the border of L_1 will not interact with the corresponding portion of L_2 and it will be simply reflected back by the substrate of the device. When I_{L_1} is below the compound system's threshold both profiles (not shown) are homogeneous. When I_{L_1} is increased above the first threshold (corresponding to region B in the left panel) we observe the formation of complex and in general nonstationary patterns resulting from the linear feedback effect of L_2's output mirror on L_1 [Fig. 2, right panel, (a),(b)].

Keeping increasing I_{L_1} the two resonators start to interact with L_2 absorbing the field emitted by L_1 (region C of left panel) and the near-field profile of both lasers is mostly dark and homogeneous except for the small portion close to the rightmost edge, due to reflection onto the substrate of L_2. By increasing the current I_{L_1} above $I_{L_1}^c$, bistable bright spots appear spontaneously [see Fig. 2, right panel, (c),(d)].

Further increase of I_{L_1} leads to the formation of generally nonstationary filaments connecting the isolated spots together. For higher values of I_{L_1} [Fig. 2, right panel, (e), (f)], corresponding to region D of the left panel), a complex pattern develops progressively through the whole transverse section. Temporally resolved detection reveals that the widely spread pattern is generally not stationary and exhibits complex dynamics.

When the parameters are set in the bistability region (region C of Fig. 2 left), the observed bright isolated spots (Fig. 2, right, C, D) are candidates for an interpretation in terms of CS, since they coexist with a homogeneous background as shown by the hysteretical behavior as a function of I_{L_1}. While they appear rather uncorrelated one to the other on the near-field images, the full demonstration of their mutual independence can only be performed by switching them on and off with a local perturbation. Indeed, it has been shown numerically that localized states in a cavity soliton laser can be switched on or off by a coherent [11,12] or incoherent [15] local optical perturbation. In our experiment, we use a coherent beam whose optical frequency is close (here, within 0.1 nm) to the emission frequency of the coupled device and whose diameter is about 15 μm. This beam is obtained from an external-cavity tunable laser in Littman configuration and applied on device L_2. By means of this local optical injection, (writing beam, WB) we are able to demonstrate independent switching of localized structures as shown on Fig. 3.

The system is prepared in the low level emission state with the parameters set in the bistable region. Starting with no spot, applying the WB to a point in the transverse plane of L_2, we generate a high intensity spot with a diameter of the order of 10 μm. We then remove the WB and the bright spot remains on indefinitely. We then apply the WB at a different position and a second spot is generated without disturbing the first one, provided the distance between the two spots is sufficient (no distance smaller than 40 μm was observed). The two spots stay on even after the WB is removed. We note that, as in previous experiments in semiconductor devices [4,7], local device inhomogeneities seem to play a role in the stabilization of localized states since although it is possible to observe stable structures in different positions, not all positions appear to be stable. We make use of this to switch off the localized structures. In experiments involving an external forcing by a holding beam, the simplest procedure is to apply a coherent local perturbation with opposite phase with respect to the holding beam. In the present case, this approach is not possible. Therefore we take advantage of mobility properties of the structures to switch them off: by applying the same pertur-

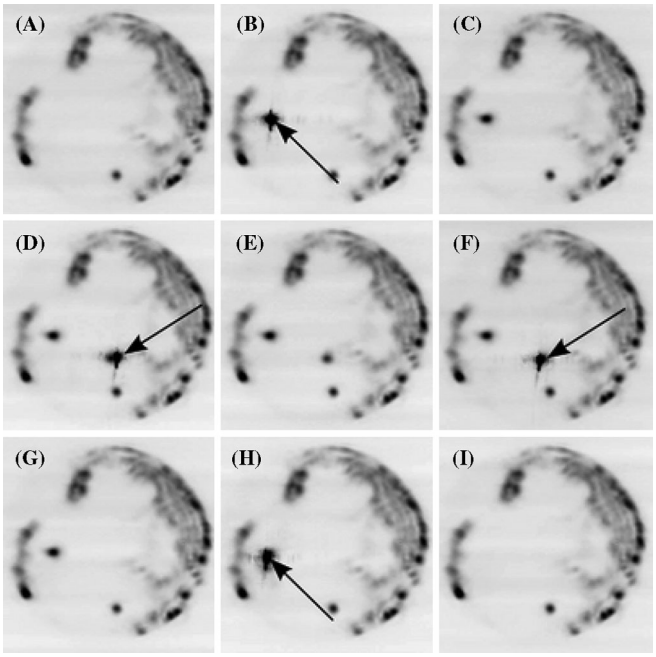

FIG. 3. L_1 near-field intensity distribution. Dark areas correspond to high intensities. Sequence of successive switching of two independent structures with an incoherent writing beam (WB) tuned at the CS wavelength with all parameter fixed. (a) Both structures are off, (b) The injection of WB switches one structure, (c) the structure remains on after the WB is blocked, (d) the injection of the WB at a second location ignites a second structure, (e) when the WB is blocked, both structures are on, (f) reapplying the WB in the vicinity of the second structure attracts it to a slightly different location, (g) when the WB is blocked the structure switches off, (h) the WB is applied in the vicinity of the first structure to attract it to a slightly different location, (i) when the WB is blocked, both structures are off.

bation as before close to a CS, we can drag it to a region of space where it is unstable and therefore switches off [Fig. 3(f) and 3(h)]. This method can be applied whenever the pinning effect of local medium inhomogeneities can be overcome by the local optical perturbation. Further more, it is also possible to switch off the structures without dragging them outside of their preferred location if the pumping current of each device is set such that the system is very close to the lower edge of the bistability region for the structure under consideration. In this case though, our optical perturbation did not appear to be sufficient to switch on a localized structure. Conversely, if the system parameter were set very close to the upper edge of the bistability region, it was not possible to switch localized structures off, except with the dragging procedure described above. While the application of the local perturbation was quasi continuous in the measurements shown above, numerical simulations performed on a model for a monolithic semiconductor laser with saturable absorber [15] indicate the possibility of ns switching time. Preliminary experimental observations indicate that perturbations as short as 100 ns (limited by the modulator) can be sufficient to switch on or off a localized structure, although no optimization (e.g., tuning and power of the writing beam) has been performed yet. The steady state of stationary CS is then reached after a rather long (hundreds of ns, depending on parameters) periodically pulsed regime at a frequency corresponding to the field roundtrip time in the longitudinal dimension of the system.

In conclusion, we have given evidence of single localized peaks that fulfill all the criteria required to be interpreted as cavity solitons in a compound semiconductor laser system with a saturable absorber. Since no injection beam is present in our experiment we believe it is a very promising realization of a semiconductor cavity soliton laser. One of the greatest strengths of this experiment is its possibly straightforward miniaturization to monolithic devices able to generate self localized, bistable and mobile laser beams. In the present version of the system, the observation of spatially localized periodically pulsed transient regimes suggests the suitability of the system to the generation of three dimensional localized structures.

This work was supported by the FET Open Project FunFACS (www.funfacs.org). We are grateful to L. Gil, L. Columbo and G. Tissoni for many useful discussions.

[1] *Dissipative solitons*, edited by N. Akhmediev and A. Ankiewicz, Lecture Notes in Physics Vol. 661 (Springer, Berlin/Heidelberg, 2005).
[2] S. Barland *et al.*, Nature (London) **419**, 699 (2002).
[3] L. Lugiato, IEEE J. Quantum Electron. **39**, 193 (2003).
[4] X. Hachair *et al.*, Phys. Rev. A **69**, 043817 (2004).
[5] F. Pedaci, P. Genevet, S. Barland, M. Giudici, and J. R. Tredicce, Appl. Phys. Lett. **89**, 221111 (2006).
[6] F. Pedaci *et al.*, Appl. Phys. Lett. **92**, 011101 (2008).
[7] Y. Tanguy, T. Ackemann, W. J. Firth, and R. Jäger, Phys. Rev. Lett. **100**, 013907 (2008).
[8] N. Rosanov and S. Fedorov, Opt. Spectrosc. **72**, 782 (1992).
[9] N. N. Rosanov, *Spatial Hysteresis and Optical Patterns* (Springer-Verlag, Berlin, Heidelberg, New York, 2002).
[10] S. V. Fedorov, A. G. Vladimirov, G. V. Khodova, and N. N. Rosanov, Phys. Rev. E **61**, 5814 (2000).
[11] M. Bache, F. Prati, G. Tissoni, R. Kheradmand, L. Lugiato, I. Protsenko, and M. Brambilla, Appl. Phys. B **81**, 913 (2005).
[12] F. Prati, P. Caccia, G. Tissoni, L. Lugiato, K. Mahmoud Aghdami, and H. Tajalli, Appl. Phys. B **88**, 405 (2007).
[13] A. J. Fischer, K. D. Choquette, W. W. Chow, H. Q. Hou, and K. M. Geib, Appl. Phys. Lett. **75**, 3020 (1999).
[14] M. Grabherr, R. Jäger, M. Miller, C. Thalmaier, J. Herlein, and K. Ebeling, IEEE Photonics Technol. Lett. **10**, 1061 (1998).
[15] K. Mahmoud Aghdami, F. Prati, P. Caccia, G. Tissoni, L. Lugiato, R. Kheradmand, and H. Tajalli, Eur. Phys. J. D **47**, 447 (2008).